Available online at www.sciencedirect.com
SCIENCE DIRECT®
Journal of Photochemistry and Photobiology A: Chemistry 165 (2004) 51–58
Journal of Photochemistry and Photobiology A:Chemistry
www.elsevier.com/locate/jphotochem

Visible light induced photocatalytic activity for degradation of acetaldehyde using transition metal incorporated Al-MCM-41 (aluminum doped silica zeolitic material)

Shalini Rodrigues, S. Uma, Igor N. Martyanov, K.J. Klabunde*

Department of Chemistry, Kansas State University, 111 Willard Hall, Manhattan, KS 66506, USA

Received 30 May 2003; received in revised form 16 October 2003; accepted 7 November 2003

Abstract

Transition metal aluminosilicates (M-Al-MCM-41) with high surface area were analyzed for photocatalytic degradation of acetaldehyde in the gas phase. The photoactivity of the catalyst under visible light irradiation is independent of the loading level of Co ions in the Co-Al-MCM-41 framework. The physical state of the transition metal oxide was characterized by XRD, IR, and diffuse reflectance studies. A high surface area with average pore diameter of 2.5 nm was obtained from BET adsorption studies. Maximal photoactivity was achieved even at low loading levels of the transition metal ion. These catalysts also exhibit good activity for degradation of acetaldehyde in the gas phase under UV light illumination.

Keywords: Mesoporous; Photocatalyst; Acetaldehyde; Al-MCM-41; Visible light irradiation; UV irradiation

1. Introduction

The vast majority of photocatalytic investigations employ TiO_2, due to its stability and low cost. However, TiO_2 requires UV light for photoreactions to proceed. To develop more light efficient catalysts it is necessary to develop new photocatalysts capable of working in the visible wavelength range. Many oxides of transition metals absorb part or all of the visible light spectrum. Thus, by doping with transition metals, TiO_2 exhibits better absorption response under visible light irradiation [1]. Mesoporous silica MCM-41 with well ordered pores in the size range of 2–10 nm, is used for a range of applications in the field of heterogeneous catalysis. Owing to the lack of active sites in the matrices of pure silica, its use as a catalyst is limited. Active sites can be generated via chemical modification, i.e. by introduction of heteroatoms into the silica matrix [2–4]. Incorporation of transition metal centers in the silicate framework can lead to improvements in its use in catalysis. There are several examples of transition metal incorporated mesoporous silicates such as Al, Ti, Cr, Fe, and Mn reported in the literature [5–9]. Transition metal (Cr, V, Fe) based titania loaded MCM-41 materials (TiO_2/Cr-Ti-MCM-41) have tested positive for degradation of organics in visible light. The chromium substituted MCM-41 was found to serve as the best support for titania to achieve the highest degradation rates of formic acid and 2,4,6-trichlorophenol [10]. M/TiO_2/SiO_2 aerogel with high surface area is also highly active for degradation of acetaldehyde utilizing visible light [11]. Fe-MCM-41 has been used for oxidation of sulfur dioxide [12]. Transition metal incorporated MCM-41 has shown unique reactivity not only for certain catalytic reactions [13] but also for photocatalytic reactions [14,15]. The recent synthesis of lanthanide incorporated MCM-41 allowed an improvement in its thermal stability and structural properties, such as pore volume and surface area in comparison with pure MCM-41 [16–19]. Yamashita et al. [20] reported that Cr-incorporated MCM-41 is effective for the photoreduction of NO in visible light, but no reports have been published on photooxidation reactions with visible light. We show for the first time that transition metal incorporated Al-MCM-41 acts as an efficient photocatalyst for degradation of gas phase acetaldehyde under visible light irradiation. Aluminosilicate zeolites with desirable cations compensating the framework charge find wide application in areas of adsorption catalysis [21–23] and nanostructure engineering [24–26]. Aluminum (Al) incorporated MCM-41, which possesses moderate Lewis acidity associated with the presence of Al in the framework position, has been claimed to be an effective hydrothermal and isomeriza-

* Corresponding author. Tel.: +1-785-532-6665; fax: +1-785-532-6666.
E-mail address: kenjk@ksu.edu (K.J. Klabunde).

1010-6030/$ – see front matter © 2004 Elsevier B.V. All rights reserved.
doi:10.1016/j.jphotochem.2003.11.010

tion catalyst [5–9,27]. For Al-MCM-41 the hydroxyl groups of the framework may serve as electron acceptors with production of hydrogen atoms. The channels/cages of these zeolites can also be modified with suitable cations by ion exchange techniques. Successful ion exchange in mesoporous silica MCM-41 has been achieved in solution. The ion exchanging site of zeolites is usually produced by substituting trivalent Al for silicon atoms. Al-MCM-41 exhibits ion exchange capacities for Na, K, and Y [28]. On the contrary, pure silica MCM-41 shows no significant levels of ion exchange [29]. Because of the equilibrium existing between the ions in solution and those within the zeolite channels, the ion exchange process is incomplete. However, this is overcome in the co-assembly route for the synthesis of transition metal doped aluminosilicates reported in the literature [30]. The process allows the direct formation of transition metal aluminosilicate having very high surface area. It is a well known fact that increasing the photocatalyst surface area is the most obvious means of improving the efficiency of photocatalytic reactions [31]. In view of this we have investigated the transition metal aluminosilicates as potential materials for photocatalysis of volatile organics. A series of the first row transition metal doped M-Al-MCM-41 were synthesized, characterized, and examined as visible light photocatalysts. Powder X-ray diffraction patterns confirmed the phase formation of the compounds. BET analysis indicated surface areas of $\sim$1000 m^2/g for the calcined samples with an average pore diameter of 2.5 nm. The transition metal was incorporated during the synthesis into the framework of the Al-MCM-41.

2. Experimental

2.1. Synthesis

Commercial diethylamine (Aldrich), cetylmethylammonium bromide (CTAB), aluminum chloride (Fisher), cobalt chloride, ammonium hydroxide (Fisher), and tetraethylorthosilcate (TEOS) (Aldrich) were used as-received for the synthesis of M-Al-MCM-41 following an earlier procedure [30]. The co-assembly process can occur involving surfactant cations, aluminosilicate species and an ammonia coordinated transition metal complex: $M(NH_3)_n^{2+}$ where M = Mn, Cr, Cu or Co and n = 4, 6. The gel has a molar composition of $1SiO_2{:}x_1Al_2O_3{:}2.5x_2\ Co^{2+}{:}20x_1NH_4OH{:}0.14CTAB{:}2.4Et_2NH{:}100H_2O$ (x_1 = 0.02 and $0.01 < x_2 < 0.05$). Synthesis of $Co_{0.05}$-Al-MCM-41 was carried out as follows: 10 ml of diethylamine solution (Et_2NH) was added to a solution containing 72 ml of deionized water, 2.04 g of cetylmethylammonium bromide, and 0.386 g of $AlCl_3{\cdot}6H_2O$ and stirred vigorously. Then 0.2689 g of $CoCl_2$ in 3.6 ml of NH_4OH (25 wt.% NH_3) was added to the above mixture. The resulting solution was stirred and to it was added 8.9 ml of tetraethylorthosilicate drop-wise. Finally the mixture was stirred at room temperature for 4 h followed by heating statically at 110 °C for 4 days in a 250 ml polypropylene container. The product was filtered, washed with water, and dried overnight at room temperature. The samples were calcined in air at 600 °C at a heating rate of 1 °C/min. The resulting product was pale yellow in color. Using the same procedure, pure Al-MCM-41 and other transition metal incorporated M-Al-MCM-41 were synthesized. Et_2NH is basic enough to form MCM-41 while also enabling the dissolution of the aluminum source, thus readily allowing incorporation of the Al^{3+} into the framework. It is this feature in the synthesis that allows the introduction of various transition metal cations into the reaction media. The use of ammonia in the procedure is to form complex cations with the transition metal ions, thus preventing precipitation under basic conditions. The most probable position of the metal ion could be at the interface of the organic and inorganic fractions. On calcination, the surfactant molecule is eventually removed and formation of a dispersed transition metal oxide phase occurs. The transition metal cations are likely to be located at the exchange sites of the MCM-41, compensating for the negative charge of the aluminosilicate framework. MCM-41 possesses regular one dimensional channels with mesopore diameters ranging from 1.6 to 10 nm. Selective doping by Al^{3+} into the framework of MCM-41 has been achieved through the co-assembly route. The possible explanation for transition metal being incorporated into Al-MCM-41 could be as follows: (a) the transition metal oxide that is formed upon calcination in air may be finely dispersed in the framework of the Al-MCM-41; (b) substitution for some of the Si or Al ions occurs, thus becoming part of the framework structure. Whatever are the sites occupied by the transition metal ions, the uniform pore size of MCM-41 is retained.

2.2. Characterization

Powder X-ray diffractograms (XRD) of the samples were recorded on a Scintag Diffractometer using a Cu Kα source. XRD was used to identify the crystal phase of the transition metal incorporated Al-MCM-41. Transition metal incorporated Al-MCM-41 powders were analyzed from 2° to 7° (2θ) with step size (0.01°) to assess the crystallinity of the samples under study. N_2 adsorption–desorption isotherms were obtained at liquid nitrogen temperature (77 K) on a NOVA apparatus. The specific surface areas were calculated according to the Brunauer–Emmett–Teller (BET) method. The pore size distributions were calculated from the desorption curves. The micropore volumes were estimated by the *t*-plot method. The surface morphology of the calcined samples were visualized using a Philip Electron Microscope operating at 100 kV (the samples were coated on a copper grid). Visible absorption spectra of the samples were recorded on a Cary 500 Scan UV-Vis NIR Spectrophotometer with an integrating sphere attachment for their diffuse reflectance in the range 200–800 nm. Infrared (IR) spectra were measured

in a Nexus FT-IR spectrometer for which the sample was mixed with KBr.

2.3. Photocatalytic studies

Photocatalytic testing, which involves the degradation of gas phase acetaldehyde, was performed in a round flat plate reactor using a 1000 W high pressure Hg lamp as light source. The combination of two VIS-NIR long pass filters (400 nm) and a colored glass filter (>420 nm) were used to eliminate ultra violet radiation while performing visible light experiments. The reaction temperature was maintained at 298 K. The reaction products were analyzed by GC-MS.

3. Results and discussion

A series of transition metal incorporated M-Al-MCM-41 was prepared by a co-assembly route, and had surface areas >1000 m^2/g. The BET surface areas, average pore diameters, and pore volumes are summarized in Table 1. It can be clearly seen that the surface areas of the transition metal incorporated M-Al-MCM-41 samples are lower when compared to pure Al-MCM-41. Nevertheless the BET surface areas of the catalysts employed in the present study are comparable to the transition metal doped M-MCM-41 (no Al). The average pore diameters change upon incorporation of transition metal.

The X-ray diffraction analyses employed to characterize the crystallinity of transition metal ion incorporated M-Al-MCM-41 samples indicated the crystal phase and crystallite sizes (about 2.5 nm). The samples studied from 2° to 7° (2θ) (Fig. 1) exhibited the same location of peaks as siliceous MCM-41 [32]. However, the intensities of the peaks are certainly lower when compared to pure siliceous MCM-41. This can be attributed to the presence of the transition metal ions during the synthesis, which can hinder the structure directing action of the template by changing the ionic strength of the medium, as reported in the literature [33]. Also, the samples when scanned from 20° to 70° (2θ) indicate the presence of the Co_3O_4 phase in addition to the silica phase (Fig. 2).

Table 1
Pore structure parameters of Co-Al-MCM-41 calculated from the adsorption branch of nitrogen adsorption isotherms

Material	A_{BET} (m^2/g)	V_{BJH} (cm^3/g)	D_{BJH} (nm)
$Co_{0.025}$-$Al_{0.04}$-MCM-41	1192	0.86	2.9
$Co_{0.050}$-$Al_{0.04}$-MCM-41	1077	0.73	2.7
$Co_{0.075}$-$Al_{0.04}$-MCM-41	1068	0.65	2.7
$Co_{0.1}$-$Al_{0.04}$-MCM-41	1074	0.68	2.7
$Co_{0.125}$-$Al_{0.04}$-MCM-41	980	0.67	2.7
$Co_{0.25}$-$Al_{0.04}$-MCM-41	910	0.64	2.9

The surface morphology was visualized using transmission electron microscopy (TEM), which was performed on a Philip Electron Microscope operating at 100 kV. The TEM micrographs exhibited channels as seen in MCM-41 and also gave the average pore diameters to be ~2.5 nm (Fig. 3). The UV-Vis spectra of the catalysts in the range 200–800 nm for various concentrations of Co^{2+} ions are shown in Fig. 4. Fig. 5 shows the spectra of pure Al-MCM-41 along with other transition metal doped samples, such as Cr, Mn, and Cu incorporated Al-MCM-41. As seen from the figure, the transition metal incorporated M-Al-MCM-41 material exhibited absorption in visible light as well as in the UV region. Significant absorption occurred in the visible range. However, no visible light absorption with pure Al-MCM-41 was observed. Co doped material showed a well defined band located at 460 nm. Also there were bands around 600–800 nm. These can be ascribed to the presence of Co^{2+}. The peak

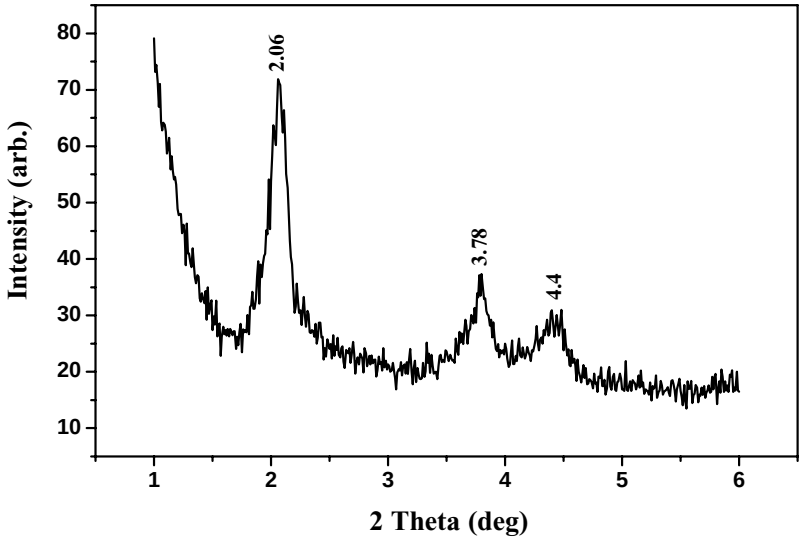

Fig. 1. X-ray powder diffraction pattern of Co-Al-MCM-41 with 0.125 mol of Co^{2+} ions. The observed peaks are due to the MCM-41 (Al incorporated) structure.

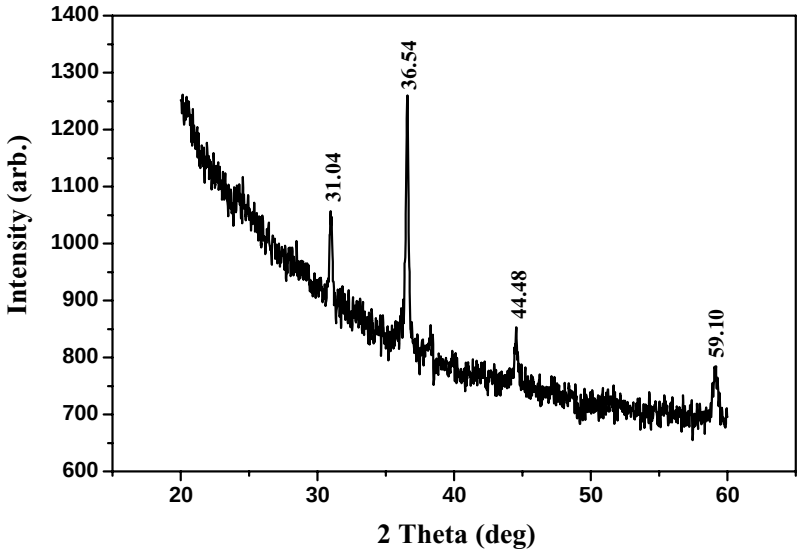

Fig. 2. X-ray diffraction patterns of Co-Al-MCM-41 with 0.25 mol of Co^{2+} ions exhibiting the Co_3O_4 phase.

~800 nm indicates cobalt oxide in the form of Co_3O_4. The absorption edges are in the vicinity of 500–600 nm. These data justify why these materials can be potential candidates for performing photochemical reactions in visible light. The absorption bands above 450 nm are mainly due to the transition metal oxide itself. In conclusion the UV-Vis study points out that there are two species, Co^{2+} and Co^{3+}, present in Co-Al-MCM-41. It is evident that the photocatalysts, employed in the present study are much different spectrally from TiO_2. It should be noted, however, that enhanced absorption of light by the catalyst is necessary, but not a sufficient condition for performing photocatalytic reactions under visible light. This is observed with Mn-Al-MCM-41, which has good absorption in the 500–600 nm regime, but fails to photodegrade acetaldehyde under visible light irradiation. The UV-Vis spectra of Cr-Al-MCM-41 shows two broad peaks at 275 and 350 nm and a shoulder at 440 nm. The bands at 275 and 350 nm are normally assigned to O → Cr^{6+} charge transfer absorption bands [33–35]. However, the d–d transition of Cr^{5+} occurs in the same spectral region [36]. Thus, the bands observed in the ultraviolet region may be due to the overlap of Cr^{5+} d–d transition and an O → Cr^{6+} charge transfer band, although the Cr^{6+} band is probably more intense. In Fig. 6, we show the infrared absorption spectra, in the range 400–1000 cm^{-1}, of Co-Al-MCM-41 calcined at 600 °C. The features that are identified in the figure (475 and 800 cm^{-1}), correspond to the vibrational modes of the oxygen (O) atom with respect to silicon (Si) atoms which they bridge, while the two well defined bands around 570 and 670 cm^{-1} have been assigned to vibrational modes of Co–O bonds in Co_3O_4 [37]. These features indicate the formation of cobalt oxide species in the calcined samples of Co-Al-MCM-41.

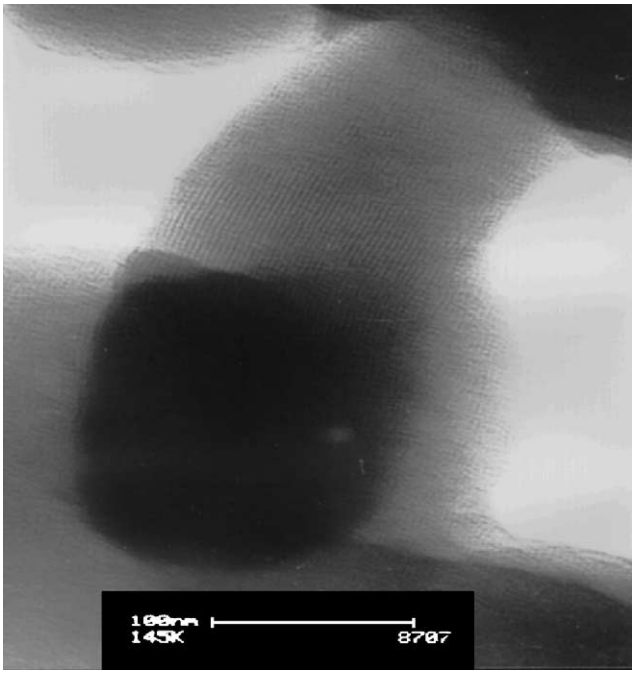

Fig. 3. TEM image of Cr-Al-MCM-41 showing channels having average pore diameters of 2.5 nm.

3.1. Photocatalytic measurements

The photoactivity of the catalysts was evaluated by measuring the loss of acetalaldehyde and the production of carbon dioxide, in the gas phase upon visible light irradiation. The procedure involved the irradiation of the sample (Co-Al-MCM-41) with visible light after adsorption–desorption equilibrium had been achieved. The irradiation source was a 1000 W Hg lamp with a 420 nm cutoff filter. One hundred microliters of acetaldehyde were added to the reactor containing the sample. The reactor

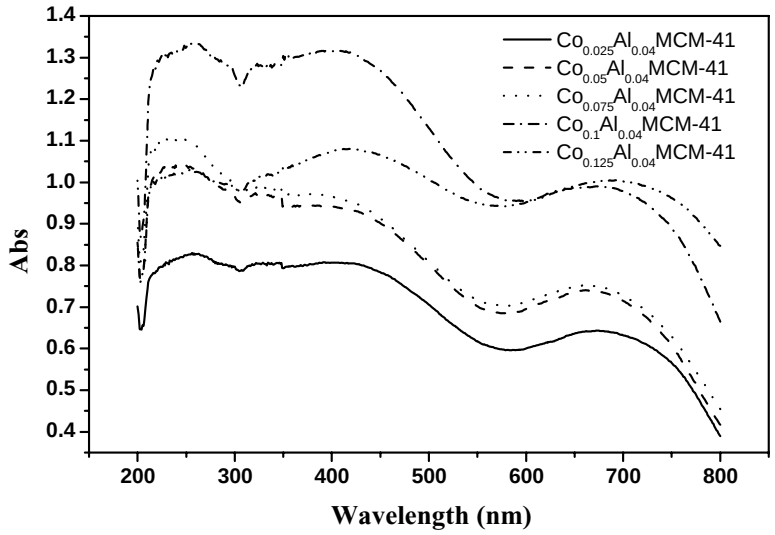

Fig. 4. UV-Vis diffuse reflectance spectra of Co-Al-MCM-41 with various concentrations of Co^{2+} ions.

was stirred constantly at a temperature of 298 K. Prior to commencing irradiation, the reaction was equilibrated for 30 min and monitored for no change in the amount of evolved acetaldehyde or CO_2. After illumination with visible light the photodegradation reaction was found to follow pseudo first order kinetics. The data were fitted to the corresponding logarithmic expression to get an apparent rate constant k in min^{-1} (Fig. 7). This rate constant is not regarded as fully interpretable since we know that a complete kinetic treatment includes substrate concentration dependence from zero to first order and other variable dependence on light intensity. Thus, k simply serves to compare relative activities of the catalysts under study. The reaction was followed by taking into consideration loss in acetaldehyde with simultaneous evolution of CO_2. It has been observed that titania supported on aluminum substituted MCM-41 produced the highest activity among the MCM-41 supports for degradation of acetophenone [38]. In the present study, photoactivity under visible light has been tested for various concentrations of Co^{2+} ions in Al-MCM-41 framework. It was observed that irrespective of the amount of Co^{2+} ions incorporated in the framework that the degradation rate constant was $0.022 \pm 0.005\ min^{-1}$. Photocatalytic reaction under UV light irradiation was also examined using a Pyrex glass cell with quartz lid. A 1000 W Hg lamp was used as light source while the cell was maintained at a constant temperature of 298 K. A 300 nm cutoff filter was used during the experiments. It is seen that the photocatalytic activity under UV light increases with an increase in concentration of Co^{2+} ions. The value of the rate constant is certainly higher for the same reaction when performed with Degussa P25 TiO_2 (Figs. 8 and 9) compared

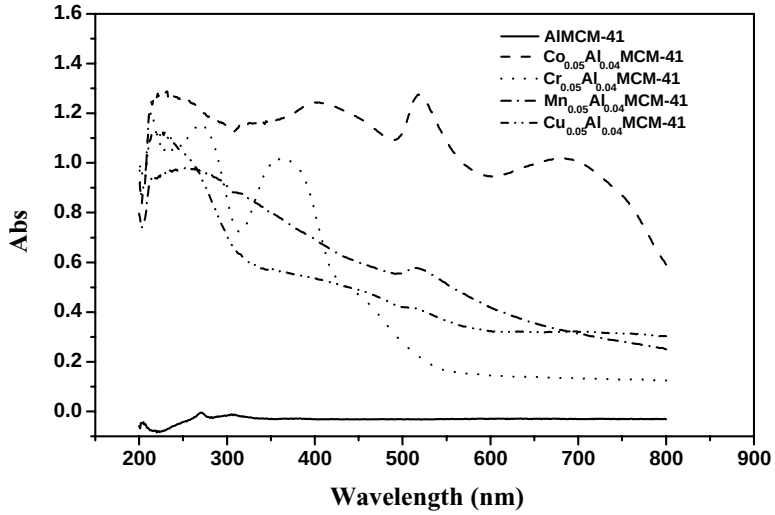

Fig. 5. UV-Vis diffuse reflectance spectra of Al-MCM-41 and M-Al-MCM-41 (M = Cr, Co, Mn, and Cu). The pure Al-MCM-41 phase does not absorb in the 380–800 nm range.

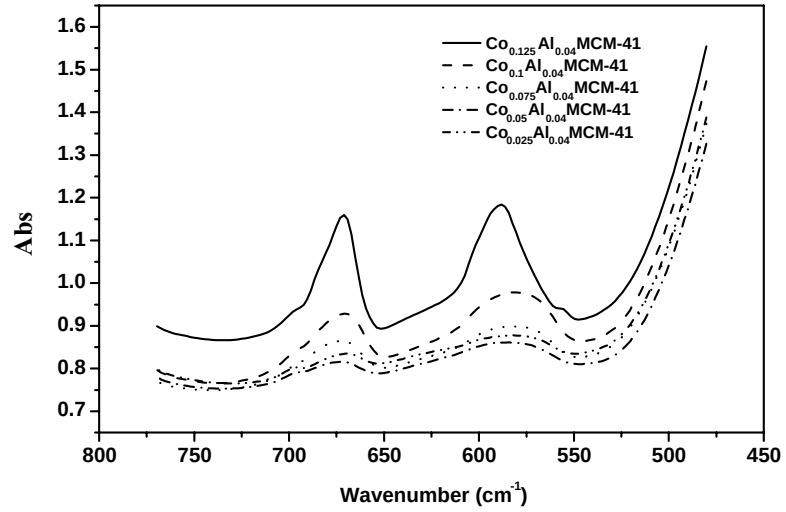

Fig. 6. IR spectra of Co-Al-MCM-41 with various concentrations of Co^{2+} ions.

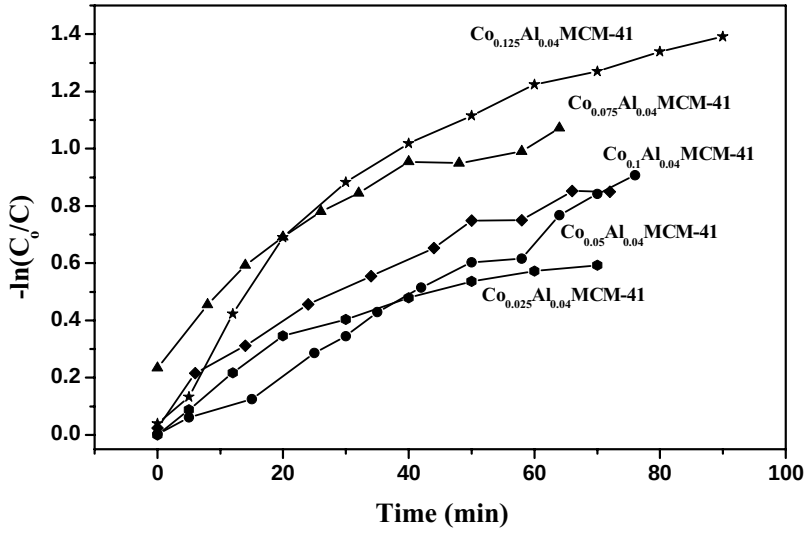

Fig. 7. Graph of $-\ln(C_o/C)$ vs. time for evolution of CO_2 using various concentrations of Co^{2+} in Co-Al-MCM-41 under visible light irradiation.

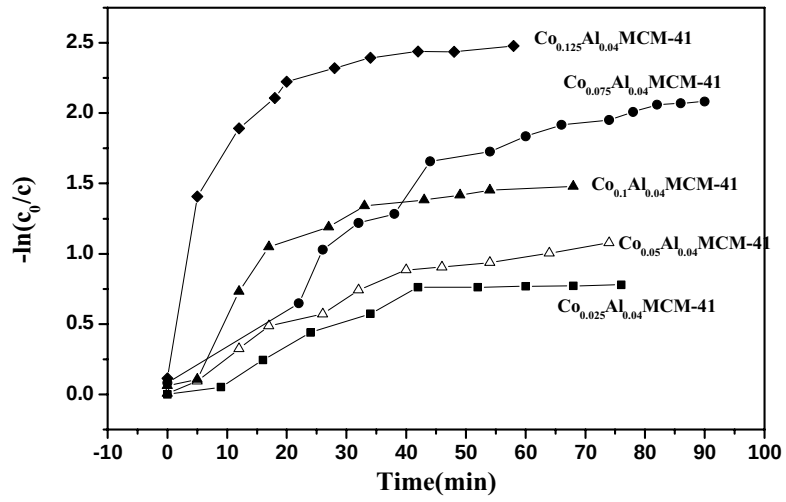

Fig. 8. Graph of $-\ln(C_o/C)$ vs. time for evolution of CO_2 using various concentrations of Co^{2+} in Co-Al-MCM-41 under UV light irradiation.

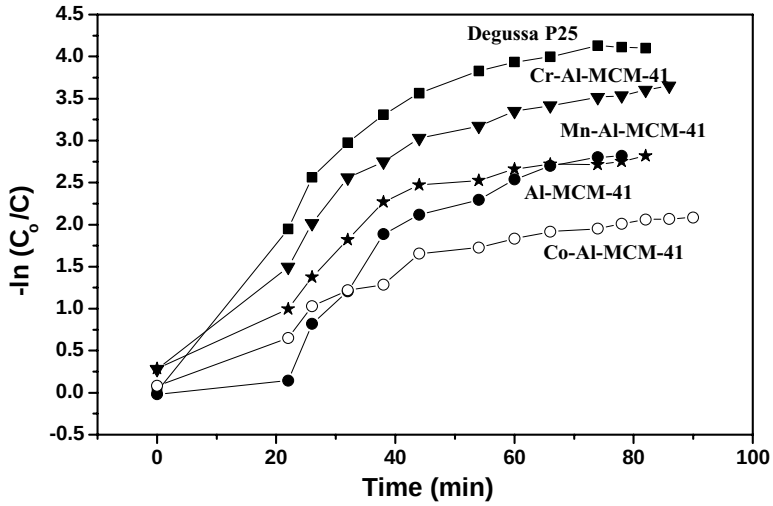

Fig. 9. Graph of $-\ln(C_o/C)$ vs. time for evolution of CO_2 using Al-MCM-41, Co-Al-MCM-41, Cr-Al-MCM-41, Mn-Al-MCM-41, and Degussa P25 TiO_2 as a standard comparison under UV light irradiation.

with the $Co_{0.125}$-$Al_{0.06}$-MCM-41. The catalysts reported herein, however, have reasonable activity both in visible and in UV light. Also, note that the Co^{2+} concentration has very little effect on k_{vis} whereas, a substantial change in the value of k_{UV} is seen for reaction under UV irradiation (Table 2). It is seen from diffuse reflectance spectra that there is absorbance even below 400 nm which might account for the increased efficiency of the catalyst under UV irradiation. Photocatalytic experiments were extended to Cr-Al-MCM-41, Mn-Al-MCM-41, and Al-MCM-41 samples. The Cr-Al-MCM-41 sample performed best among the transition metal incorporated M-Al-MCM-41 for the gel composition where $x_2 = 0.02$. In the case of Cr-Al-MCM-41, the photoactivity probably arises due to the presence of Cr^{3+}/Cr^{6+} redox couple in the catalyst. Such a phenomenon is also observed for Cr/TiO_2/MCM-41 in the photodegradation of 2,4,6-trichlorophenol under visible light irradiation [10]. Thus, it has been observed that the Co-oxide or Cr-oxide moieties in Al-MCM-41 can exhibit efficient photocatalytic reactivity for degradation of acetaldehyde under visible light as well as UV irradiation. This photocatalytic system with finely dispersed transition metal oxide moieties on mesoporous Al-MCM-41 seems to be a good candidate, especially for degradation of organic volatile compounds.

Table 2
Rate constant for CH_3CHO degradation under visible and UV light using various transition metal incorporated M-Al-MCM-41

Material	k_{CO_2} (min^{-1}) visible light	k_{CO_2} (min^{-1}) UV light
$Co_{0.025}$-$Al_{0.04}$-MCM-41	0.014	0.022
$Co_{0.050}$-$Al_{0.04}$-MCM-41	0.024	0.035
$Co_{0.075}$-$Al_{0.04}$-MCM-41	0.026	0.02
$Co_{0.100}$-$Al_{0.04}$-MCM-41	0.025	0.042
$Co_{0.125}$-$Al_{0.04}$-MCM-41	0.026	0.098
Cr-Al-MCM-41	0.016	0.068
P25	Nil	0.085

4. Conclusions

The results of the present study underline the unique properties of M-Al-MCM-41 as visible light photocatalysts for degradation of organic volatile compounds, along with the capability of Al-MCM-41 to act as support which prevents the growth of large crystallites of transition metal oxide. The XRD data suggests the formation of a well dispersed Co_3O_4 phase along with the pure phase of Al-MCM-41. The catalysts reported herein, however, have reasonably good activity both in visible and in UV light. The Cr-Al-MCM-41 sample performed best among the transition metal incorporated M-Al-MCM-41 for the gel composition where $x_2 = 0.02$ under UV light as reported in the present study.

Acknowledgements

The support of the U.S. Army Research Office (ARO) through a MURI contract (DAAD19-01-1-0619) is acknowledged with gratitude.

References

[1] Y. Sakata, T. Yamamoto, T. Okazaki, H. Imamura, T. Tsuchiya, Chem. Lett. (1998) 1253.
[2] A. Corma, Chem. Rev. 97 (1997) 2373.
[3] S. Biz, M.L. Occelli, Catal. Rev.-Sci. Eng. 40 (1998) 329.
[4] A. Sayari, Chem. Mater. 8 (1996) 1840.
[5] O.N. Le, R.T. Thomas, US Patent 5,232,580 (1993).
[6] A. Corma, M.T. Navarro, J.P. Pariente, J. Chem. Soc., Chem. Commun. (1994) 147.

[7] H. Kosslick, G. Lischke, G. Walther, W. Storek, A. Martin, R. Fricke, Microporous Mater. 9 (1997) 13.
[8] F. Rey, G. Shankere, T. Mashmeyer, J.M. Thomas, R.G. Bell, Top. Catal. 3 (1996) 121.
[9] J.M. Thomas, Faraday Discuss. 100 (1995) C9.
[10] L. Davydov, E.P. Reddy, P. France, P.G. Smirniotis, J. Catal. 203 (2001) 157.
[11] J.Q. Wang, S. Uma, K.J. Klabunde, Appl. Catal. B. 48 (2004) 151.
[12] A. Wingen, N. Anastasievic, A. Hollnagel, D. Werner, F. Schuth, J. Catal. 193 (2000) 248.
[13] B. Notari, Adv. Catal. 41 (1996) 253.
[14] M. Anpo, M. Che, Adv. Catal. 44 (1999) 119.
[15] H. Yamashita, J. Zhang, M. Matsuoka, M. Anpo, in: M. Anpo (Ed.), Photofunctional Zeolites, Nova Science Publishers Inc., New York, 2000, p. 129.
[16] N.H. He, L. Bao, Q.H. Xu, Stud. Surf. Sci. Catal. 105 (1997) 85.
[17] W. Zhang, T.J. Pinnavaia, J. Chem. Soc., Chem. Commun. (1998) 1185–1186.
[18] A.S. Araujo, M. Jaroniec, J. Colloid Interface Sci. 218 (1999) 462.
[19] A.S. Araujo, M. Jaroniec, Stud. Surf. Sci. Catal. 129 (2000) 187.
[20] H. Yamashita, K. Yoshizawa, M. Ariyuki, S. Higashimoto, M. Che, M. Anpo, J. Chem. Soc., Chem. Commun. (2001) 435.
[21] S. Chatterjee, H.L. Greene, J.Y. Park, J. Catal. 138 (1992) 179.
[22] W. Grunert, N.W. Hayes, R.W. Joyner, E.S. Shipro, M.R.H. Siddiqui, G.N. Baeva, J. Phys. Chem. 98 (1994) 10832.
[23] J. Connerton, R.W. Joyner, M. Stockenhuber, J. Chem. Soc., Chem. Commun. (1997) 187.
[24] M.D. Baker, J. Godber, G.A. Ozin, J. Phys. Chem. 89 (1985) 2299.
[25] G.D. Stucky, J.E. MacDougall, Science 247 (1990) 669.
[26] C.-G. Wu, T. Bein, Science 264 (1994) 1757.
[27] A. Corma, A. Martinez, V. Martinez-Soria, J.B. Monton, J. Catal. 153 (1995) 25.
[28] J.M. Kim, J.H. Kwak, S. Jun, R. Ryoo, J. Phys. Chem. 99 (1995) 16742.
[29] A. Poppl, M. Harmann, L. Kevan, J. Phys. Chem. 99 (1995) 17251.
[30] W. Lin, Q. Cia, W. Pang, Yue, J. Chem. Soc., Chem. Commun. (1998) 2473.
[31] G. Dagan, M. Tomikiewicz, J. Phys. Chem. 97 (1993) 12651.
[32] A. Sayari, P. Liu, M. Kruk, M. Jaroniec, Chem. Mater. 9 (1997) 2499.
[33] Z.D. Zhu, Z.X. Chang, Kevan, J. Phys. Chem. 103 (1999) 2680.
[34] P. McCarthy, J. Lauffenburger, P. Skonezny, D. Pohrer, Inorg. Chem. 20 (1981) 1566.
[35] J.S.T. Mambrim, H.O. Pastore, C.U. Davanzo, E.J.S. Vichi, O. Nakamura, Vagus, Chem. Mater. 5 (1993) 166.
[36] C.D. Garner, J. Kendrick, P. Lambert, F.E. Mabbs, H. Hillier, Inorg. Chem. 15 (1976) 1287.
[37] H.D. Lutz, Feher, Spectrochim. Acta A 27 (1971) 357.
[38] Y. Xu, C. Langford, J. Phys. Chem. 101 (1997) 3115.